Zeitschrift: Schweizerische mineralogische und petrographische Mitteilungen = Bulletin suisse de minéralogie et pétrographie

Band: 71 (1991)

Heft: 2

Artikel: Relics of high pressure metamorphism in the Lepontine Alps (Switzerland) : 40Ar/39Ar and microprobe analyses on white K-micas

Autor: Hammerschmidt, Konrad / Frank, Eric

DOI: https://doi.org/10.5169/seals-54361

SCHWEIZ. MINERAL. PETROGR. MITT. 71, 261–274, 1991

Frau Prof. Dr. Emilie Jäger gewidmet

Relics of high pressure metamorphism in the Lepontine Alps (Switzerland) – $^{40}Ar/^{39}Ar$ and microprobe analyses on white K-micas

by *Konrad Hammerschmidt*[1] and *Eric Frank*[2]

Abstract

Microprobe and $^{40}Ar/^{39}Ar$ isotope data are reported for metamorphic white K-mica from granitic rocks, sampled along a NW–SE profile of increasing meso-Alpine metamorphism from greenschist facies (400 °C; 2–3 kb) to the upper staurolite zone (600 °C; 6–8 kb) in the Lepontine Alps, Switzerland. The phengite content (up to 7.2 Si per formula unit) and the 3T polytype of white K-mica in the assemblage muscovite-biotite-K-feldspar-quartz reveals a formation pressure of ~13 kb, reflecting conditions of the eo-Alpine metamorphism. With increasing meso-Alpine metamorphic grade a systematic evolution of white K-mica composition from phengite to muscovite can be observed. Electron microprobe analyses of single mica grains reveal large compositional variations in Si-content indicating chemical disequilibrium. Thus the random distribution of high Si-contents reflects relics of the high pressure eo-Alpine event.

With increasing meso-Alpine metamorphism the white K-mica composition evolved from phengite to muscovite. Local disequilibrium led to randomly distributed domains of high Si-content – even within one single muscovite grain.

The age spectra of these white K-micas are hump-shaped with the highest apparent ages (up to 25 Ma) at medium degassing temperatures. With increasing metamorphic grade, the hump-shaped age spectra diminish and at metamorphic temperatures of 600 °C the age spectrum of the muscovite (KAW 201) gives a well-defined plateau age of 14.0 ± 0.3 Ma, interpreted as a cooling age. Prior Rb–Sr and K–Ar age determinations on biotite of these rocks gave age values of 10–14 Ma, which are widespread in the Lepontine Alps. K–Ar ages of white micas from the Mesozoic calcareous schists in this area also fall in the same age range. We conclude that, phengitic components in the white K-mica of the granitic rocks formed during the eo-Alpine metamorphism survived the meso-Alpine temperatures of 400–500 °C in the NW part of the investigated cross-section. In contrast, the white K-micas of the calcareous schists of the same area are completely equilibrated due to the meso-Alpine event.

Keywords: $^{40}Ar/^{39}Ar$ data, K-mica, Alpine metamorphism, Lepontine Alps, Switzerland.

Introduction

Stepwise $^{40}Ar/^{39}Ar$ age spectra of thermally altered minerals of contact aureoles have allowed valuable insights into the thermal effects associated with igneous intrusions on the resetting of K–Ar ages (Berger, 1975; Hanson et al., 1975; Harrison and McDougall, 1980).

In polymetamorphic terrains also, $^{40}Ar/^{39}Ar$ ages of minerals have turned out to be a very successful tool for elucidating the effects of different thermal events, for understanding the processes of mineral age resetting and mineral reequilibration (e.g. Chopin and Monie, 1984; Dallmeyer and Gee, 1986; Wijbrans and McDougall, 1986), and for testing theoretical models of distributed diffusion domain sizes (Lovera et al., 1989).

In this paper, we consider a suite of polymetamorphic granitic rocks and their white K-micas collected along a NW–SE profile of increasing metamorphic grade in the Lepontine Alps, Switzerland. Here we find the unique opportunity to study the influence of Barrow-type Alpine metamorphism from lower greenschist facies through to the upper staurolite zone on the chemical composition of white micas and on the age resetting behaviour of

[1] FU Berlin, Institut für Mineralogie, FR Geochemie, Boltzmannstrasse 18–20. D-1000 Berlin 33.
[2] Bundesamt für Energiewirtschaft, HSK, CH-5303 Würenlingen.
This work was possible using the facilities at the Physikalisches Institut, Sidlerstrasse 5, CH-3012 Bern and at the Abt. für Isotopengeologie, Erlachstrasse 9a, CH-3012 Bern.

these minerals as a function of increasing metamorphic grade. Using microprobe and $^{40}Ar/^{39}Ar$ analyses, we re-investigated white micas from a metamorphic profile between Brig and Verampio (Fig. 1) which has been studied previously by PURDY and JÄGER (1976). Due to similar closure temperatures for both K/Ar-white mica and Rb/Sr-biotite systems, we anticipate similar ages in a regional metamorphic but cooling terrain. However, near Brig the K/Ar ages on white K-micas are a factor of two greater than the biotite ages: behaviour attributed to the possible influence of excess argon by PURDY and JÄGER (1976).

To date, the significance of these high ages remains unclear. Two main possibilities must be considered for this paradox. Firstly, higher ages may be due to the presence of excess or inherited radiogenic argon. Alternatively, these phengites may have been overprinted by at least two if not several metamorphic events with only partial and incomplete resetting of the K–Ar isotope system. In order to distinguish between these possibilities detailed $^{40}Ar/^{39}Ar$ incremental release analyses and microprobe analyses were performed on five samples selected from the cross-section Brig to Verampio (KAW 400, 401, 164, 165, and 201 of Fig. 2).

Geological setting

STRUCTURAL FEATURES

The study area is located in the western part of the Lepontine Alps and extends from Brig to Verampio where the lower Pennine nappes are exposed (Fig. 1). These units represent the deepest tectonic elements of the Central Alps and consist of intensively folded pre-Triassic basement rocks (mainly granitic and quartz feldspatic gneisses, paraschists and amphibolites) which are separated from each other by strongly squeezed Mesozoic cover rocks (calcareous schists and marbles). According to HALL (1972) and MILNES (1974), one of the most characteristic structural features in this area is the complex large-scale folding suffered by the nappe units subsequent to their initial emplacement. At least three phases of major post-nappe folding can be distinguished. The earliest post-nappe folds

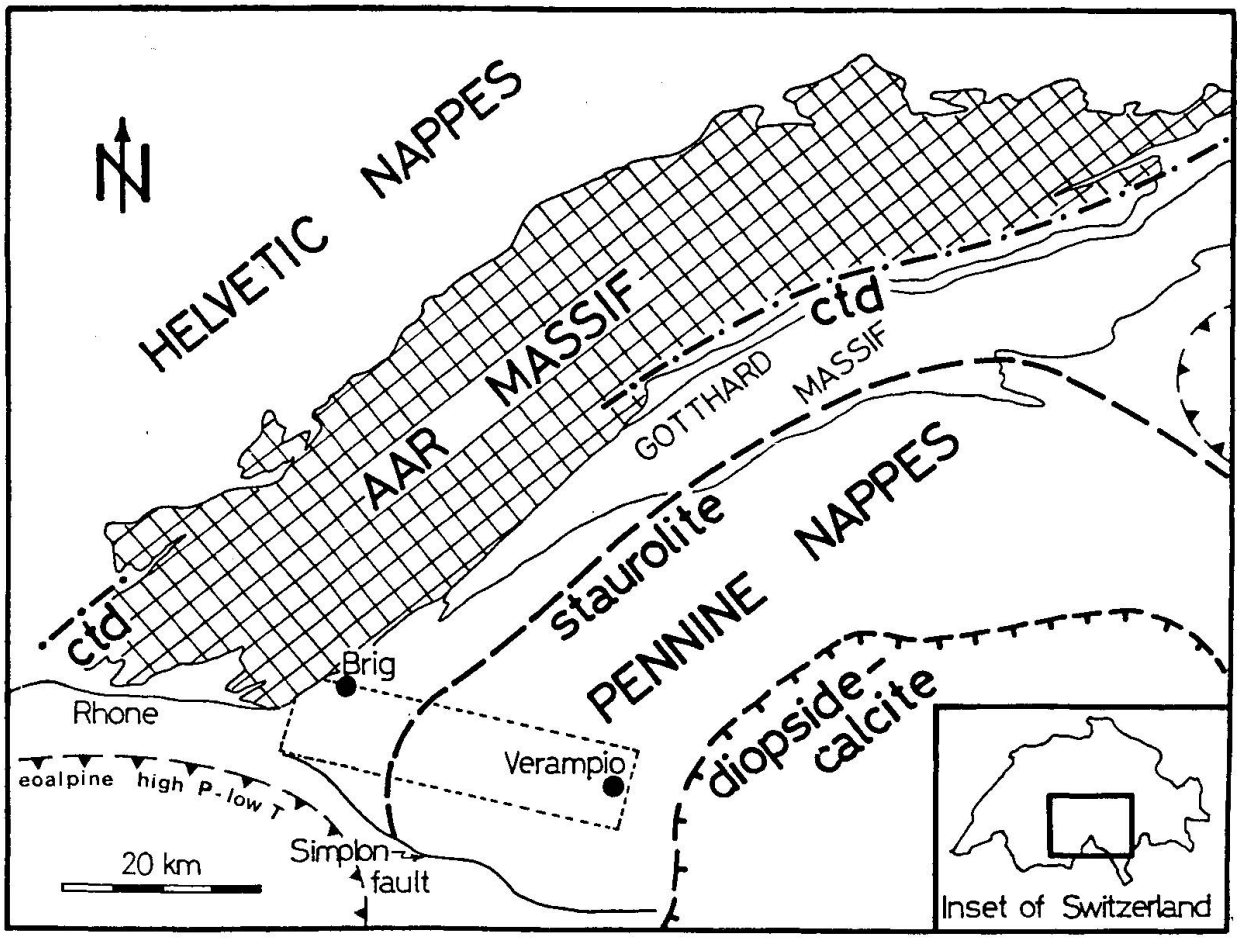

Fig. 1 Tectonic sketch map of the Central Alps, showing the location of the study area. Alpine metamorphic zone boundaries according to FREY and WIELAND (1978), NIGGLI and NIGGLI (1965), and TROMMSDORFF (1966), refering to the first appearence of chloritoid (ctd), staurolite, and diopside-calcite. The box indicates the investigated area.

were essentially isoclinal and were accompanied by a strong schistosity which is the main foliation in this area. Later, two successive phases of back-folding led to the present overall structure (MILNES et al., 1981). According to STECK (1987) the emplacement of the gneissic folds and nappe-folds took place mainly in a ductile shear zone underneath a large overburden of up to 20–30 km thickness. The western margin of the area is marked by the late-stage Simplon fault, characterised by mylonites and cataclasites, which reflect post-metamorphic displacement movements.

METAMORPHIC HISTORY

According to a number of recent investigations it is now well established that the Alpine orogeny had at least two distinct metamorphic phases (FREY et al., 1974; TRÜMPY, 1980): an eo-Alpine high-pressure event of late Cretaceous age, followed by a high temperature regime during the mid-Tertiary (meso-Alpine metamorphism). In the study area no petrological or geochronological evidence of an eo-Alpine high-pressure metamorphism has been found to date. On the other hand, the zones of the meso-Alpine metamorphism are well documented in the area from Brig to Verampio, and show a systematic increase in grade from greenschist to higher amphibolite facies (NIGGLI and NIGGLI, 1965; FREY and WIELAND, 1978; Frank, 1979) which crosscuts the tectonic units. Detailed investigations of the metamorphic conditions (FRANK, 1983) of the Mesozoic rocks in the cross-section have shown a systematic increase in pressure and temperature from about 400–420 °C at 2–3 kb (Brig) up to 580–620 °C at 6–8 kb (Verampio).

PREVIOUS GEOCHRONOLOGICAL INVESTIGATIONS

Many isotope mineral age data are available from this area. Concordant U/Pb monazite ages from the Verampio granite of 20 Ma indicate that high-temperature conditions of the meso-Alpine phase prevailed until this time in the southern part of the cross-section (KÖPPEL and GRÜNENFELDER, 1978). Quite recently, VANCE and O'NIONS (1991) reported age values of 29 and 26 Ma for the core and the rim of garnets from Mesozoic rocks indicating meso-Alpine metamorphism began at least 29 Ma ago. Much younger Rb/Sr biotite ages from granitic rocks and K/Ar mica ages from the Mesozoic cover rocks (8–13 Ma) have also been reported reflecting the timing of the closure temperatures for Sr and Ar (HUNZIKER and BEARTH, 1969).

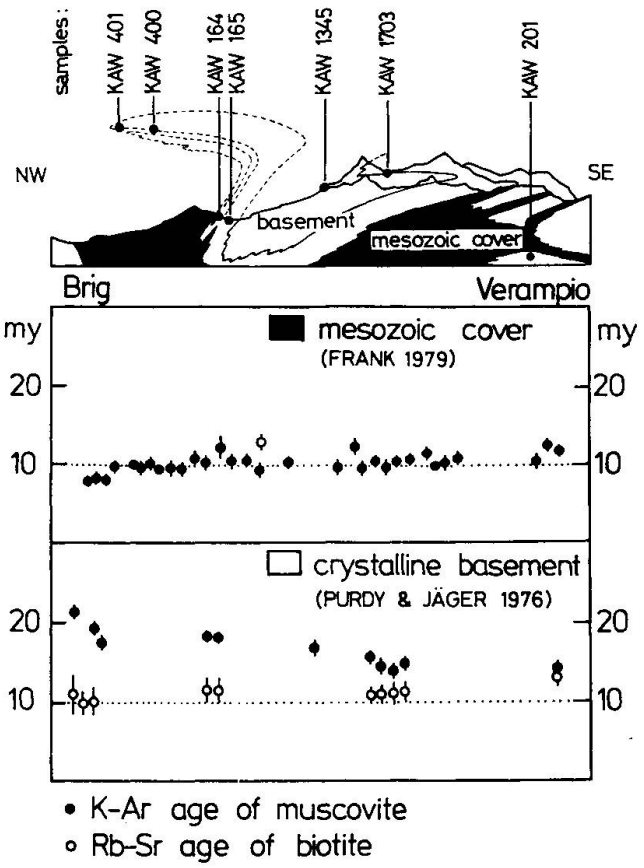

Fig. 2 Summary of apparent mica ages in two different rock types along the cross-section from Brig to Verampio; data from FRANK (1979) and PURDY and JÄGER (1976). Samples analysed (KAW 401 to KAW 201) in this study are shown in the schematic structural profile.

In figure 2 the regional distribution pattern of K/Ar muscovite and Rb/Sr biotite ages along the cross-section from Brig to Verampio is summarized, and represents apparent mica ages in two different rock types (Mesozoic cover rocks = calcareous schists; crystalline basement rocks = granite gneisses). In the cover rocks conventional K/Ar muscovite ages of 8–13 Ma are found along the whole cross-section. Incremental $^{40}Ar/^{39}Ar$ release analyses on two muscovite samples yielded well defined plateau ages of 9.0 and 11.8 Ma (FRANK and STETTLER, 1979).

These ages are interpreted as cooling ages, reflecting the time when the rocks cooled below the temperature range critical for argon retention. In spite of the significant change in metamorphic grade along this cross-section, all muscovites were closed to Ar loss at about the same time indicating a more or less horizontal "cooling isotherm" cutting the steeply inclined metamorphic isograde-surfaces (FRANK, 1983). This implies a differential uplift and cooling regime along the cross-section, beginning with faster cooling rates in the SE and

Tab. 1 Chemical compositions (% wt) and structural formulae for white K-mica from the profile Brig to Verampio.

KAW	401	401	164	164	165	165	1345	1345	201	201
SiO_2	51.70	48.60	47.98	49.80	47.10	48.60	48.00	47.90	45.80	45.98
Al_2O_3	22.10	25.80	28.50	26.30	24.90	24.80	29.70	29.80	29.20	29.00
FeO	6.30	6.29	4.15	3.60	7.20	6.70	4.70	4.50	5.68	5.49
MnO	0.00	0.11	0.00	0.10	0.00	0.00	0.00	0.00	0.00	0.00
MgO	3.30	2.51	2.52	3.10	2.70	2.80	1.45	1.25	1.30	1.30
CaO	0.00	0.19	0.10	0.00	0.00	0.00	0.00	0.00	0.00	0.00
Na_2O	0.02	0.11	0.15	0.20	0.11	0.20	0.20	0.22	0.30	0.30
K_2O	11.30	11.10	10.90	11.00	10.89	10.90	11.50	11.60	10.60	10.80
TiO_2	0.60	0.40	0.49	0.43	0.71	0.98	0.37	0.30	0.86	0.93
Total	95.32	95.11	94.78	94.53	93.60	94.97	95.91	95.57	93.74	93.80
Si	7.07	6.69	6.54	6.77	6.63	6.71	6.49	6.50	6.37	6.39
Al^{iv}	0.93	1.31	1.46	1.23	1.37	1.29	1.51	1.50	1.63	1.61
Al^{vi}	2.63	2.87	3.11	2.98	2.75	2.74	3.22	3.26	3.15	3.13
Ti	0.06	0.04	0.05	0.04	0.07	0.10	0.04	0.03	0.09	0.10
Fe^{2+}	0.72	0.72	0.47	0.41	0.84	0.77	0.53	0.51	0.66	0.63
Mn		0.01		0.01						
Mg	0.67	0.51	0.51	0.63	0.56	0.57	0.29	0.25	0.27	0.26
oct. occ.	4.08	4.15	4.14	4.07	4.22	4.18	4.08	4.05	4.17	4.12
Ca		0.03	0.01							
Na	0.01	0.03	0.04	0.05	0.03	0.05	0.05	0.06	0.08	0.08
K	1.97	1.95	1.89	1.91	1.96	1.92	1.98	2.00	1.88	1.91
int.lay.	1.98	2.01	1.94	1.96	1.99	1.97	2.03	2.06	1.96	1.99

calculated on the basis of 22 oxygens per formula unit and with the tetrahedral sites beeing completely filled by Si^{iv} and Al^{iv}. The white K-micas of sample KAW 401 show 3T and $2M_1$ polytype and all the other samples show $2M_1$ polytype.

much slower cooling in the NW at Brig thus pointing to a post-metamorphic updoming of the deepest tectonic units – the Verampio complex.

For both isotope systems (K/Ar-white mica and Rb/Sr-biotite), similar closure temperature of about 300 ± 50 °C has been estimated (JÄGER et al., 1967). In the granitic basement rocks the Rb–Sr biotite age pattern, ranging from 10 to 12 Ma, is consistent with the cooling ages found in the Mesozoic cover rocks (Fig. 2). However, significantly higher K–Ar ages are found for coexisting phengite in these gneissic samples, where ages up to 22 Ma can be observed. In the northwestern part of the cross-section, the age discrepancy between coexisting biotite and phengite is up to 12 Ma. With increasing metamorphic grade, the white mica K–Ar ages decrease and become concordant with the Rb–Sr ages of coexisting biotite as well as with the K–Ar muscovite ages of the Mesozoic rocks.

Microprobe studies

CHEMICAL COMPOSITION OF THE WHITE K-MICAS

Compositions of white K-mica were obtained by microprobe analyses for the assemblage white

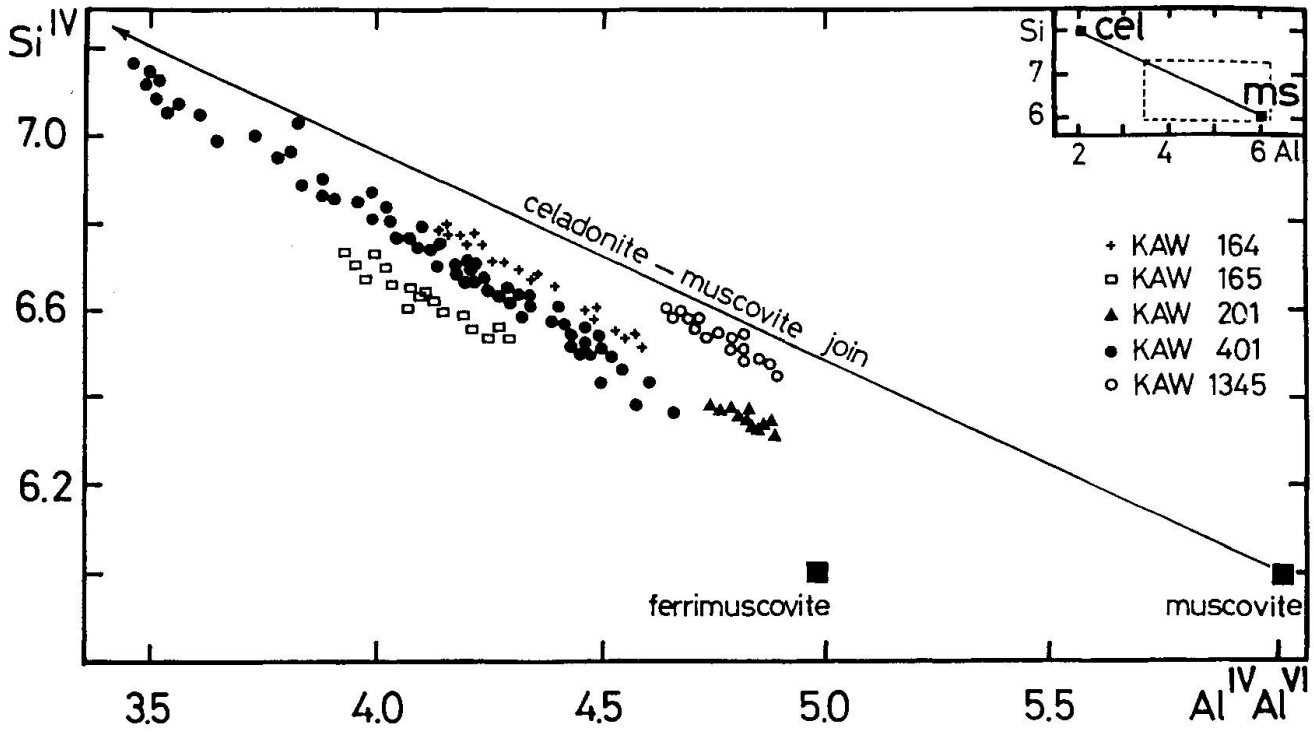

Fig. 3 Correlation of tetrahedral Si versus total Al with respect to the endmembers muscovite, ferrimuscovite and celadonite.

K-mica-biotite-potassic feldspar-plagioclase + qz. This assemblage can be followed in the granitic basement rocks along the whole cross-section from NW to SE, from lower greenschist to higher amphibolite facies. In order to trace the chemical evolution of the white K-mica as a function of increasing metamorphic grade, detailed microprobe analyses were performed on the samples shown in figure 2. Some selected geochemical data for typical mica compositions from the cross-section are given in table 1, with all data summarized in a Si vs Al_{tot} diagram (Fig. 3) and in terms of the Si-content (Fig. 7).

The lower grade samples (KAW 401, 164, and 165) are essentially muscovite-celadonite solutions with minor components of ferrimuscovite and paragonite. In sample KAW 401 Si-contents range up to 7.20 pfu (per formula unit) which is close to phengite, a species defined as intermediate between muscovite and celadonite (Guidotti and Sassi, 1976). The Si vs Al_{tot} correlation in figure 3 points to a Tschermak substitution (Fe, Mg) Si = $Al^{vi}Al^{iv}$. In sample KAW 401 strong chemical variations can be observed within the scale of one thin section, with Si ranging from 6.30 up to 7.20 (pfu). Detailed microprobe analyses on two mica flakes permitted contouring of the Si-content which reveals that strong chemical variations can be observed even on the scale of a single mineral grain (Fig. 4). Irregular Si-distribution patterns with random or sometimes concentric Si variations reflect local domains of reequilibration.

Considering the close textural relationship of phengite to biotite (Fig. 5) the Si-contours may reflect a "frozen in" reaction texture, where one of the reactant phases has been exhausted. Equilibration must have been restricted to local domains. The most likely exchange reaction has been biotite + phengite I + potassic feldspar + quartz + water = phengite II, a reaction which was recently investi-

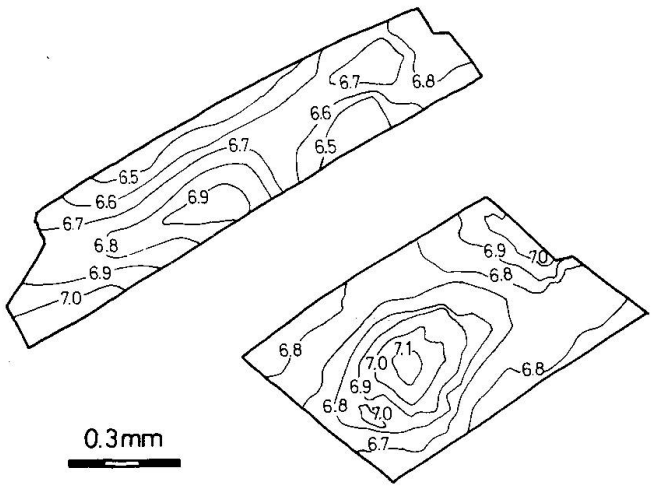

Fig. 4 Si-contours in two white K-mica flakes, reflecting relic domains of high phengite content; plane perpenticular to (001). Sample KAW 401.

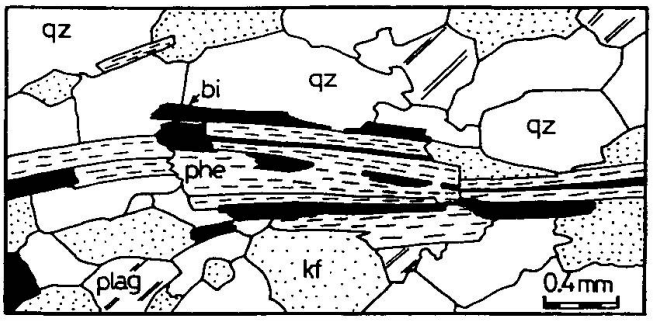

Fig. 5 Textural relationship between phengitic mica (phe), biotite (bi), and the matrix minerals quartz (qz), K-feldspar (Kf), and plagioclase (plag). In sample KAW 401 relics of biotite can be observed overgrown by phengite.

gated experimentally by MASSONNE and SCHREYER (1987).

EVOLUTION OF THE P,T-PATH

The meso-Alpine metamorphic grade increased from 400–420 °C at 2–3 kbar (Brig) to 580–620 °C at 6–8 kbar (Verampio). As can be deduced from figures 3 and 7 the Si- or celadonite-content as well as the extent of the Tschermak substitution are clearly related to metamorphic grade, reflecting a chemical evolution of phengite towards muscovite as a function of increasing metamorphic temperature and pressure.

In the limiting assemblage phengite-biotite-potassic feldspar-quartz, the compositions of white K-mica are uniquely defined by the p,T-conditions and by a_{H_2O}. These data may therefore be used to trace the evolution of possible p,T-paths. An interpretation for the large compositional variations of Si in sample KAW 401 (Si 6.3 to 7.2) is discussed in figure 6. In this p,T-diagram the stability limits of the Si-phengites for the limiting assemblage phe-bi-kf-qz are shown based on the experimental data of MASSONNE and SCHREYER (1987). The results of sample KAW 401 indicate that this rock originally experienced high pressure conditions (p ~13 kbar) at eo-Alpine time and was subsequently overprinted at slightly higher temperatures and lower pressures (meso-Alpine), which reduced the Si from 7.2 to 6.3. Obviously, under meso-Alpine metamorphic conditions disequilibrium must have been an important phenomena, locally preserving the high Si-contents. In the higher grade samples at Verampio (KAW 201) the results indicate that we have reached the stability field of muscovite with complete chemical equilibration. This chemical evolution of white K-mica along the cross-section has important implications for the interpretation of the K–Ar age results.

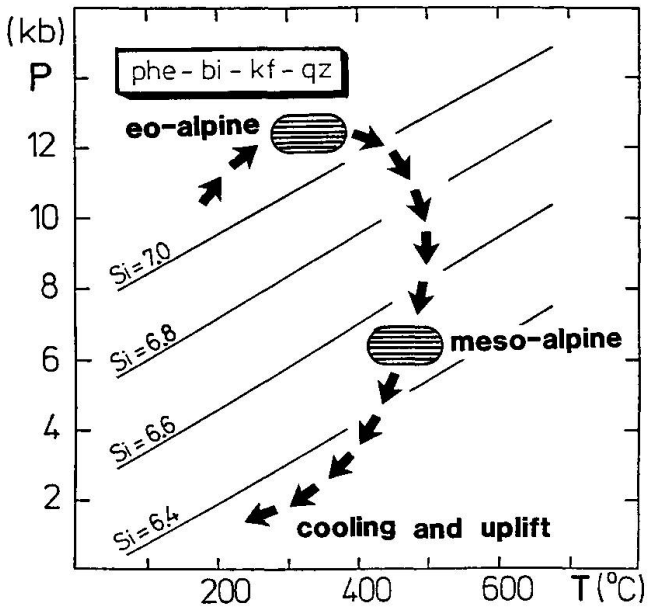

Fig. 6 Compilation of stability curves for phengites with different Si-contents in the limiting assemblage phengite-biotite-potassic feldspar-quartz according to MASSONNE and SCHREYER (1987). A possible p,T-path is shown which can be deduced from the variation of si-content in sample KAW 401.

$^{40}Ar/^{39}Ar$ analyses

METHOD

Five samples, together with six monitors (Be 4 M), were irradiated using the fast neutron facilities at the Kernforschungszentrum Karlsruhe, BRD. Sample weights were between 8 and 14 mg. Sample preparation for irradiation and extraction, neutron fluence measurements, Ar extraction and gas purification have been described previously (HAMMERSCHMIDT, 1982; HURFORD and HAMMERSCHMIDT, 1985). The integrated mean fluence of neutrons with energies above 0.1 MeV was about $6.0 \cdot 10^{17}$ n_f cm^{-2}. The fluence inhomogeneity over all samples was found to be smaller than 1.6%. With argon standards the reciprocal sensitivity of the mass spectrometer was determined as $(5.691 \pm 0.080) \cdot 10^{-12}$ cm^3 STP^{40} Ar/mV. At blank measurements the $^{39}Ar/^{41}Ar$ ratio of about 0.85 was typical for hydrocarbons. The amount of mass 41 increased to a maximum value of $8.0 \cdot 10^{-13}$ cm^3 Ar-equivalents. In the temperature range between 600 and 1300 °C the hydrocarbon contribution to mass 39 was always less than 0.03%. The blank measurements were made for the whole extraction procedure and included the gas load from the extraction line and mass spectrometer. For temperatures less than 1200 °C extraction blanks were typically $2.5 \cdot 10^{-10}$ cm^3 STP ^{40}Ar, and increased to

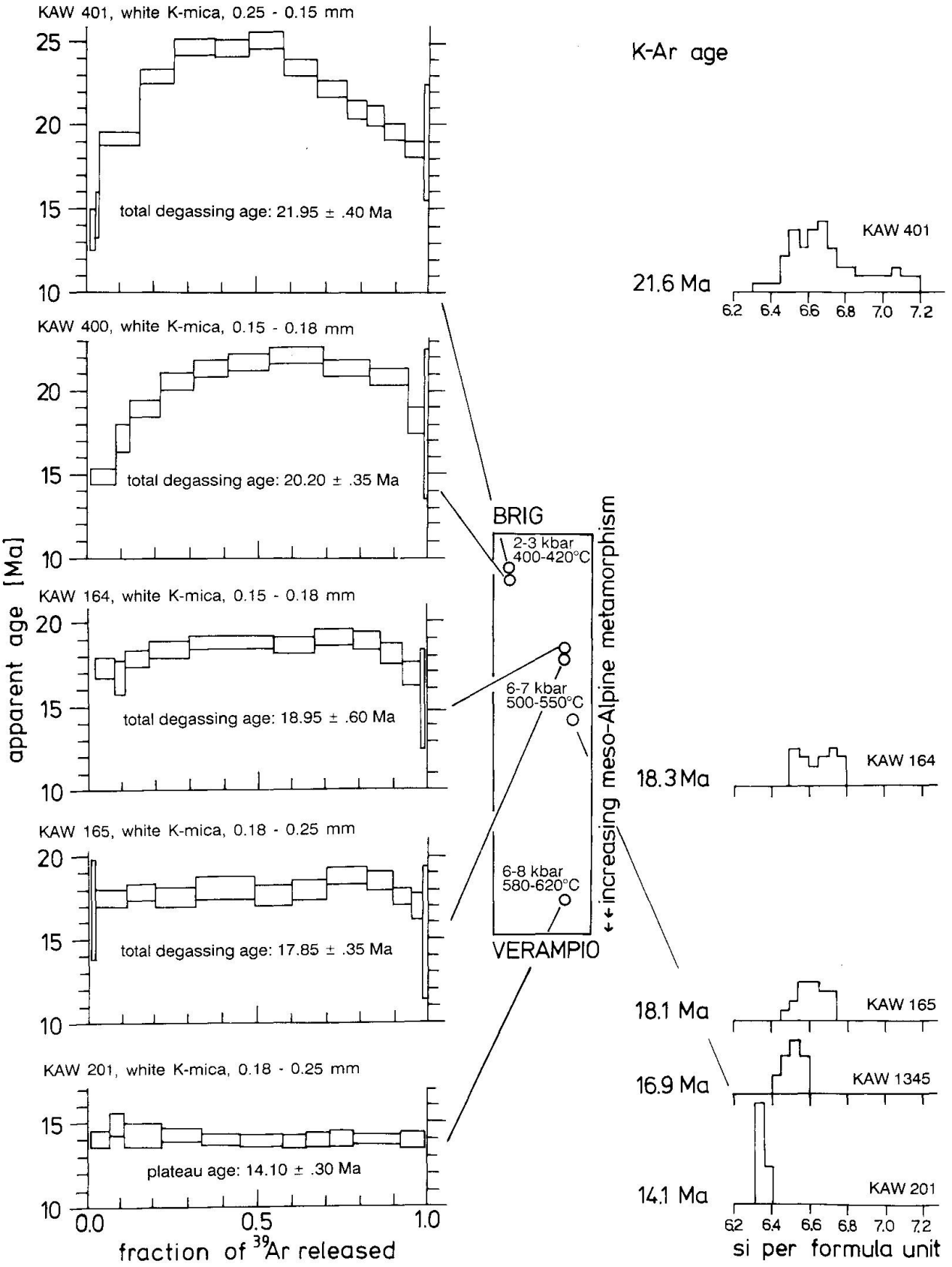

Fig. 7 The age spectra of the investigated samples in the metamorphic profile from Brig to Verampio. The rectangle shows the geographical relationship of the samples. The metamorphic conditions are from FRANK (1983). The K/Ar ages are given by PURDY and JÄGER (1976). The higher the Si-content of the micas the larger the celadonit component of the micas. With increasing metamorphic grade and with decreasing Si-content the hump-shaped spectra diminish and results in a plateau age of 14.0 ± 0.3 Ma (KAW 201) interpreted as a cooling age.

Tab. 2 $^{40}Ar/^{39}Ar$ analytical step degassing data for white K-mica from the profile Brig to Verampio.

Temp. °C	^{40}Ar x10^{-8}cm^{3}STP/g	$^{40}Ar/^{36}Ar$	$^{39}Ar/^{37}Ar$	$^{36}Ar/^{38}Ar_{(Cl)}$	rad/tot	$^{10}Ar^*/^{39}Ar_{(K)}$	age (Ma)
KAW 401, white K-mica, 150-250 µm, Gebidem, 13.59 mg							
615	9.10 ± 1.30	354 ± 40	19.60 ± 1.20	1.30 ± 0.30	0.165	2.60 ± 1.50	13.0 ± 8.0
695	6.41 ± 0.60	444 ± 70	144 ± 30	3.46 ± 0.50	0.334	1.95 ± 0.80	10.0 ± 4.0
745	5.81 ± 0.70	970 ± 350	98.5 ± 10.0	1.23 ± 0.40	0.696	2.45 ± 0.50	12.5 ± 2.5
805	11.23 ± 0.60	1312 ± 310	157 ± 15	5.70 ± 1.35	0.774	2.85 ± 0.30	14.6 ± 1.4
860	103.6 ± 1.6	1935 ± 80	282 ± 30	1.685 ± 0.070	0.847	3.770 ± 0.060	19.20 ± 0.40
915	90.3 ± 1.5	3510 ± 290	365 ± 20	0.795 ± 0.065	0.916	4.513 ± 0.080	22.95 ± 0.45
940	115.0 ± 2.1	3935 ± 330	225 ± 10	0.440 ± 0.040	0.925	4.860 ± 0.090	24.70 ± 0.50
965	98.0 ± 1.80	3290 ± 250	201.0 ± 7.5	0.300 ± 0.020	0.910	4.848 ± 0.090	24.65 ± 0.50
995	115.5 ± 2.1	1405 ± 45	209.5 ± 12.0	1.312 ± 0.040	0.790	4.929 ± 0.090	25.05 ± 0.55
1030	90.40 ± 1.70	3460 ± 310	203.5 ± 11.0	0.441 ± 0.040	0.915	4.616 ± 0.080	23.45 ± 0.50
1055	71.93 ± 1.30	4355 ± 580	268.0 ± 17.0	0.430 ± 0.060	0.932	4.361 ± 0.080	22.20 ± 0.50
1085	44.50 ± 1.00	3450 ± 580	171.0 ± 13.0	0.328 ± 0.050	0.914	4.117 ± 0.100	20.95 ± 0.60
1100	42.40 ± 0.90	2910 ± 440	1050 ± 300	1.25 ± 0.18	0.899	4.058 ± 0.110	20.65 ± 0.60
1140	47.20 ± 0.90	4780 ± 1000	700 ± 100	1.00 ± 0.20	0.938	3.864 ± 0.090	19.65 ± 0.50
1250	46.16 ± 0.90	4780 ± 1100	250.5 ± 10.0	0.74 ± 0.17	0.938	3.650 ± 0.090	18.60 ± 0.50
1800	18.2 ± 1.0	443 ± 100	13.40 ± 0.50	13.7 ± 1.5	0.334	3.75 ± 0.90	19.1 ± 3.5
Total	916.0 ± 13.7	2256 ± 95	203.7 ± 10.0	0.816 ± 0.090		4.319 ± 0.060	21.95 ± 0.40
KAW 400, white K-mica, 150-180 µm, Nanztal, 10.25 mg							
690	26.15 ± 0.80	326 ± 30	21. 0 ± 1.9	5.4 ± 1.1	0.096	2.4 ± 1.7	12.5 ± 8.0
755	5.10 ± 0.80	450 ± 130	12.05 ± 0.40	1.65 ± 0.40	0.351	1.97 ± 1.20	10.0 ± 6.0
815	56.80 ± 1.20	1040 ± 55	11.08 ± 0.08	1.80 ± 0.09	0.716	2.91 ± 0.09	14.85 ± 0.50
860	30.40 ± 0.90	1635 ± 250	155.0 ± 14	1.16 ± 0.17	0.819	3.36 ± 0.16	17.10 ± 0.80
900	67.35 ± 1.30	2430 ± 250	267 ± 12	1.00 ± 0.10	0.878	3.710 ± 0.090	18.90 ± 0.50
930	81.10 ± 1.50	2130 ± 150	520 ± 50	2.18 ± 0.16	0.861	4.035 ± 0.090	20.55 ± 0.50
960	84.15 ± 1.60	4725 ± 750	408 ± 25	0.571 ± 0.090	0.938	4.185 ± 0.080	21.30 ± 0.50
1000	102.0 ± 2.00	4030 ± 475	310 ± 13	0.335 ± 0.040	0.927	4.265 ± 0.080	21.70 ± 0.50
1035	130.6 ± 2.20	6365 ± 900	450 ± 25	0.400 ± 0.050	0.954	4.350 ± 0.070	22.10 ± 0.45
1080	110.7 ± 1.90	6470 ± 1100	1130 ± 150	0.59 ± 0.10	0.954	4.185 ± 0.070	21.20 ± 0.45
1150	95.15 ± 1.70	4660 ± 660	5000 ± 2500	0.83 ± 0.11	0.937	4.085 ± 0.070	20.80 ± 0.45
1250	33.75 ± 1.00	3690 ± 1200	950 ± 300	0.41 ± 0.13	0.920	3.57 ± 0.15	18.20 ± 0.80
1850	21.2 ± 0.9	429 ± 80	200 ± 100	12.5 ± 2.0	0.312	3.54 ± 0.90	18.0 ± 4.5
Total	844.4 ± 13.0	2170 ± 140	103 ± 11	1.11 ± 0.10		3.967 ± 0.060	20.20 ± 0.35
KAW 164, white K-mica, 180-250 µm, Gantergneis, 10.11 mg							
525	70 ± 20	358 ± 19	2.2 ± 1.2	0.20 ± 0.03	0.173	16.0 ± 4.5	80 ± 20
650	135 ± 30	337 ± 20	0.83 ± 0.40	0.162 ± 0.002	0.124	12.5 ± 5.0	64 ± 20
710	10.65 ± 0.90	360 ± 60	6.80 ± 0.90	0.154 ± 0.040	0.180	4.1 ± 2.9	21 ± 15
750	3.60 ± 0.90	690 ± 390	20.5 ± 3.0	0.150 ± 0.080	0.574	3.0 ± 1.6	15.5 ± 8.0
830	56.7 ± 1.4	990 ± 60	155.0 ± 8.0	0.710 ± 0.035	0.702	3.40 ± 0.12	17.30 ± 0.60
855	23.7 ± 1.3	1865 ± 400	132.0 ± 11	0.225 ± 0.050	0.842	3.27 ± 0.20	16.70 ± 1.0
910	53.5 ± 1.8	2370 ± 340	178.0 ± 8.0	0.265 ± 0.035	0.875	3.51 ± 0.10	17.85 ± 0.60
955	83.9 ± 3.0	3190 ± 460	209.5 ± 9.0	0.229 ± 0.025	0.908	3.61 ± 0.08	18.40 ± 0.50
1000	196.5 ± 4.0	2880 ± 350	267.0 ± 8.0	0.202 ± 0.011	0.897	3.69 ± 0.07	18.80 ± 0.40
1035	93.7 ± 4.0	2350 ± 320	181.0 ± 10	0.180 ± 0.013	0.874	3.66 ± 0.09	18.65 ± 0.50
1070	102.0 ± 2.5	1480 ± 90	280 ± 15	0.614 ± 0.03	0.801	3.76 ± 0.10	19.10 ± 0.50
1105	60.7 ± 1.3	2030 ± 210	507 ± 70	3.10 ± 0.30	0.855	3.71 ± 0.10	18.90 ± 0.55
1140	49.0 ± 1.1	4050 ± 1000	860 ± 200	1.05 ± 0.25	0.927	3.56 ± 0.10	18.15 ± 0.60
1200	35.2 ± 1.0	5525 ± 2500	560 ± 100	0.65 ± 0.30	0.947	3.31 ± 0.12	16.90 ± 0.70
1285	7.1 ± 1.0	2220 ± 2150	45.5 ± 4.0	0.20 ± 0.20	0.867	3.01 ± 0.60	15.4 ± 3.0
1870	9.8 ± 1.0	390 ± 70	10.1 ± 1.0	0.91 ± 0.70	0.241	3.4 ± 3.0	17 ± 15
Total	993.9 ± 40	982.8 ± 55	71.2 ± 7.5	0.21 ± 0.10		3.720± 0.070	18.95 ± 0.60
KAW 165, white K-mica, 180-250 µm, Eistengneis, 12.37 mg							
605	16.4 ± 1.3	314 ± 16	6.80 ± 0.50	0.9 ± 0.3	0.059	1.8 ± 1.5	9.0 ± 7.5
665	27.60 ± 0.80	322 ± 12	14.70 ± 1.80	2.5 ± 0.4	0.080	5.45 ± 2.40	28 ± 10
730	6.45 ± 0.70	495 ± 90	34.75 ± 4.00	0.68 ± 0.13	0.403	3.05 ± 1.00	15.5 ± 5.0
760	9.10 ± 0.75	645 ± 110	45.75 ± 4.50	0.66 ± 0.11	0.542	3.30 ± 0.60	16.8 ± 3.0
835	80.1 ± 1.9	1220 ± 60	143.0 ± 5.5	0.682 ± 0.025	0.758	3.430 ± 0.090	17.45 ± 0.50
880	64.2 ± 1.8	2000 ± 160	134.5 ± 2.0	0.387 ± 0.030	0.852	3.51 ± 0.10	17.85 ± 0.50
920	114.2 ± 4.5	1640 ± 100	92.0 ± 3.0	0.334 ± 0.013	0.820	3.45 ± 0.11	17.55 ± 0.60
950	135.8 ± 6.5	900 ± 35	72.7 ± 3.5	0.478 ± 0.025	0.672	3.56 ± 0.13	18.10 ± 0.70
980	84.35 ± 3.00	1805 ± 135	176 ± 30	0.292 ± 0.016	0.836	3.46 ± 0.11	17.65 ± 0.60
1020	79.80 ± 3.00	1915 ± 170	117 ± 10	0.306 ± 0.018	0.846	3.53 ± 0.12	17.95 ± 0.60
1055	100.7 ± 1.8	1215 ± 50	226 ± 11	1.01 ± 0.04	0.757	3.69 ± 0.08	18.80 ± 0.50
1085	60.15 ± 0.80	1850 ± 140	565 ± 60	1.21 ± 0.09	0.840	3.64 ± 0.09	18.55 ± 0.50
1135	44.65 ± 0.80	2330 ± 300	690 ±100	1.65 ± 0.20	0.873	3.43 ± 0.10	17.50 ± 0.50
1215	26.05 ± 0.80	2460 ± 570	550 ± 90	0.84 ± 0.20	0.880	3.33 ± 0.15	16.95 ± 0.80
1860	14.40 ± 0.80	450 ± 80	53.3 ± 7.5	1.45 ± 0.90	0.344	3.44 ± 0.80	15.6 ± 4.0
Total	864 ± 10	1155 ± 35	131.0 ± 7.0	0.582 ± 0.50		3.506 ± 0.060	17.85 ± 0.35

KAW 201, white K-mica, 180-250 μm, Verampio, 11.97 mg

675	101.3 ± 1.6	332 ± 5.5	11.4± 2.5	11.9 ± 1.0	0.109	20.7 ± 2.5	103 ± 20
805	11.20 ± 0.70	350 ± 50	215 ± 100	70 ± 20	0.156	2.0 ± 2.0	10 ± 10
845	53.75 ± 1.00	714 ± 25	780 ± 110	7.50 ± 0.25	0.586	2.76 ± 0.09	14.05 ± 0.50
870	50.30 ± 1.00	519 ± 15	1380 ± 620	12.25 ± 0.40	0.430	2.93 ± 0.14	14.95 ± 0.70
910	94.8 ± 4.5	775 ± 35	580 ± 60	5.65 ± 0.17	0.618	2.80 ± 0.14	14.30 ± 0.70
945	85.75 ± 1.80	975 ± 30	425 ± 35	2.64 ± 0.09	0.696	2.805 ± 0.060	14.30 ± 0.40
980	69.5 ± 1.3	1650 ± 90	415 ± 25	1.40 ± 0.08	0.820	2.750 ± 0.060	14.00 ± 0.35
1010	66.2 ± 1.3	2410 ± 220	430 ± 35	0.78 ± 0.07	0.877	2.730 ± 0.060	13.95 ± 0.35
1045	47.6 ± 1.0	1195 ± 80	525 ± 80	3.08 ± 0.20	0.753	2.710 ± 0.080	13.85 ± 0.45
1080	43.65 ± 0.95	1770 ± 180	2600 ± 1400	2.08 ± 0.20	0.833	2.730 ± 0.080	13.90 ± 0.45
1150	42.30 ± 0.95	1700 ± 170	4700 ± 4400	5.04 ± 0.50	0.826	2.740 ± 0.090	14.00 ± 0.50
1160	86.70 ± 1.5	1880 ± 110	3900 ± 1600	1.65 ± 0.10	0.843	2.740 ± 0.060	13.95 ± 0.30
1220	39.20 ± 0.90	2530 ± 410	4000 ± 3500	2.13 ± 0.35	0.883	2.720 ± 0.090	13.90 ± 0.50
1380	18.30 ± 0.80	345 ± 40	45 ± 15	25.4 ± 2.5	0.143	3.90 ± 1.9	20.0 ± 9.5
Total	810 ± 13	815 ± 20	546 ± 75	4.2 ± 2.0		2.813 ± 0.050	14.34 ± 0.30

J-value = 0.002837 ± 28

$^{39}Ar(K)$ = neutron induced only from K

I.U.G.S.constants (Steiger and Jäger,1977)

Be 4M muscovite standard:

K = 8.70 ± 0.05 % (Purdy and Jäger, 1976)

t = 18.5 ± 0.2 Ma (Flisch, 1982)

$^{36}Ar/^{37}Ar(Ca) = (2.7 \pm 0.2) * 10^{-4}$

$^{38}Ar/^{37}Ar(Ca) = (6.0 \pm 2.0) * 10^{-5}$ (Stettler et al.,1973)

$^{39}Ar/^{37}Ar(Ca) = (6.8 \pm 0.2) * 10^{-4}$

$^{40}Ar/^{37}Ar(Ca) = (3.0 \pm 3.0) * 10^{-4}$ (Turner et al.,1973)

$^{38}Ar/^{39}Ar(K) = (1.4 \pm 0.3) * 10^{-2}$ (Maurer, 1973)

$^{40}Ar/^{39}Ar(K) = (6.0 \pm 2.0) * 10^{-3}$ (Stettler et al.,1973)

$5.2 \cdot 10^{-10}$ cm³ STP ^{40}Ar. For masses 36, 38, 39 the blanks were $9.0 \cdot 10^{-13}$ cm³ STP, for masses 35 and 37 of the order of $2.2 \cdot 10^{-13}$ cm³ STP (in ^{40}Ar equivalents). The values listed in the table were corrected for blanks, Ar interferences from neutron reaction with Ca and K, and for neutron fluence inhomogeneity. The errors given in the table are at the 95% confidence level and include all error sources except those of the decay constants and the uncertainties of the standard itself. Recommended ratios and constants were used for age calculations (Steiger and Jäger, 1977).

RESULTS AND DISCUSSION

$^{40}Ar/^{39}Ar$ analyses are reported in table 2. The results of argon isotope determinations are shown in age spectrum diagrams, where the apparent ages are plotted versus the cumulative fraction of ^{39}Ar released (Fig. 7). The age spectra of the samples correlate to the increasing meso-Alpine metamophic grade. The samples KAW 401, 400, 164, and 165 exhibit hump-shaped age spectra; the apparent ages increase with successive incremental heating steps to a maximum apparent age at medium degassing temperatures, and then decrease in the following heating steps. With increasing meso-Alpine metamorphic grade the hump of the age spectra is less pronounced and disappears in sample KAW 201, which yields a plateau age of 14.0 ± 0.3 Ma as given by 88% of ^{39}Ar released. This age is in the same range as the K/Ar and $^{40}Ar/^{39}Ar$ ages of the white K-mica from the Mesozoic cover rocks and the Rb/Sr biotite ages from the granitic gneisses of the basement rocks. Since the regional age pattern crosscuts tectonic units as well as reaction isograde the ages are interpreted as cooling ages (Purdy and Jäger, 1976); Frank and Stettler, 1979; Frank, 1983).

The temperature of the heating step which corresponds to the maximum age of the spectrum is called the maximum differential age temperature (T_{mda}). The T_{mda} varies in a systematic manner. In sample KAW 401 T_{mda} appears at 995 °C where 57.9% of ^{39}Ar is released. For samples KAW 400, 164, and 165 the T_{mda} varies between 1035 °C, 1070 °C, and 1055 °C for an increasing percentage of ^{39}Ar released – 68.7%, 78.8%, and 81.6%, respectively. The hump-shaped producing component shifts to more retentive places in the white K-micas, and with increasing metamorphic grade diminishes its influence on the age spectra.

In samples KAW 401, 400, and 165 the first few temperature steps yield apparent ages of 11 ± 2 Ma related to a ^{39}Ar release of 1.8%, 1.04%, and 0.3%, respectively. These ages are geologically significant, because they are concordant with the K–Ar muscovite and Rb–Sr biotite ages found in the investigated region (Purdy and Jäger, 1976; Jäger et al., 1967; Frank, 1979).

In sample KAW 164 and 201 the first steps show high apparent ages up to 103 Ma with 0.3% and 1.13% ^{39}Ar released. This may be due to an excess

component or, more likely, a small amount (0.3–1.13%) of ^{39}Ar transferred from less retentive lattice sites to more retentive ones by ^{39}Ar recoil.

In general, disturbed age spectra for which the apparent ages are too old, are suspected of having suffered Ar recoil or having excess Ar. However, the total degassing ages of KAW 401, 400, 164, 165 and 201 amounting to 21.95 ± 0.40 Ma, 20.20 ± 0.35 Ma, 18.95 ± 0.60, 17.85 ± 0.35 Ma, and 14.35 ± 0.30 Ma respectively, are identical compared to the conventional K/Ar ages of 21.6 Ma, 19.4 Ma, 18.3 Ma, 18.1 Ma, and 14.1 Ma within the error limits of 3% (PURDY and JÄGER, 1976). It appears that either radiogenic nor neutron produced ^{39}Ar loss occurred during the irradiation. Using the conversion factor $1.932 \cdot 10^{-11}$ cm^3 ^{39}Ar/ppm K the potassium content calculated from the $^{40}Ar/^{39}Ar$ data are identical to those given by PURDY and JÄGER (1976), which also support that ^{39}Ar loss, generated by recoil effects due to neutron irradiation as reported by FOLAND et al. (1984) on sheet silicates (glauconites) seems to be negligible. Due to theoretical considerations, JESSBERGER (1982) has pointed out that even for moderate temperatures (150–400 °C) during irradiation the expected diffusion losses exceed the ^{39}Ar recoil loss for a given grain size. However, the effective diffusion path will not be identical with the physical grain size; rather it will be controlled by subgrain boundaries, density of linear dislocations, exsolution interfaces and planar effects such as stacking faults. Some of these effects and their consequences for $^{40}Ar/^{39}Ar$ age spectra are discussed by HARRISON and FITZ GERALD (1986), ONSTOTT and PEACOCK (1987) and ROSS and SHARP (1988). HESS and LIPPOLT (1986) have reported loss and redistribution of ^{39}Ar due to recoil where the losses are < 0.5% for biotites with low and non-stoichiometric K contents (< 7%). Recoil effect does not play a major role to cause the hump-shaped age spectra in our samples for several reasons. First, the grain size of the samples between 0.15 and 0.25 mm exceeds an average recoil distance of about $0.1 \cdot 10^{-3}$ mm (HUNNECKE and SMITH, 1976). Moreover, all the samples have the same grain size and all should have suffered nearly the same ^{39}Ar loss. Finally, the amount of ^{39}Ar recoil loss would require approx. 50% to explain the age difference of ~12 Ma (KAW 401). Such an amount is far greater than the loss reported for micas (HESS and LIPPOLT, 1986).

Therefore, excess or inherited argon most likely explains the age discrepancy between the mica ages from the two lithologies. Excess argon can be discriminated in a $^{39}Ar/^{40}Ar$ vs $^{36}Ar/^{40}Ar$ diagram. The implications and advantages of this diagram have been discussed by RODDICK et al. (1980), GILLESPIE et al. (1983, 1984), and RADICATI DI BROZOLO et al. (1981), and critically commented upon by DALRYMPLE et al. (1988). The ordinate intercept ($^{39}Ar/^{40}Ar$) reflects the age of the sample, which should correspond to the plateau age of the age spectrum. The abscissa intercept represents the trapped Ar component which has been incorporated during the mineral growth. Generally, this trapped component has an atmospheric $^{40}Ar/^{36}Ar$ ratio of 295.5 and due to the variable amount of the endmembers (the trapped and the age component) in each heating step, the data points fall on a binary mixing line; deviations from the athmospheric ratio indicates excess argon.

Now, we make use of the correlation diagram to look for excess argon and to trace the evolution from the hump-shaped to the plateau age spectrum. For this purpose three samples were selected again according to the increasing grade of metamorphism. The data points for KAW 401, 164, and 201 are represented in figure 8. The data of the most pronounced hump-shaped age spectrum (KAW 401) show no correlation in this diagram which implies a heterogenous ^{40}Ar excess component of variable $^{40}Ar/^{36}Ar$ composition which decreases the $^{39}Ar/^{40}Ar$ ratio. Basically, the data points of the samples KAW 400 and KAW 165 point to the same behaviour. Therefore a simple mixing line between two endmembers – the age and an excess component – does not exist and the scatter of the data points may be explained by an inherited argon component which is only partially degassed during the meso-Alpine event. We consider that the high pressure mineral phase phengite which is found in domains within the mica flakes is a possible candidate for retaining inherited argon from an older – eo-Alpine – high pressure event. In some of these samples the meso-Alpine metamorphic temperature exceeded 500 °C. This temperature was not high enough or did not persist long enough to completely reset the white micas.

In sample KAW 164 the age spectrum is rather flat and the heating steps between 995 °C and 1140 °C yield a straight line, intersecting the abscissa at a $^{36}Ar/^{40}Ar$ ratio of $2.655 \cdot 10^{-3}$ which corresponds to a $^{40}Ar/^{36}Ar$ ratio of 377 ± 25, indicating a homogeneously distributed ^{40}Ar excess component. The ordinate intercept gives an age value of 17.9 ± 0.5 Ma – too high compared to the K–Ar white K-mica ages from the Mesozoic schists and the Rb–Sr biotite ages (10–12 Ma) from the crystalline basement of the same area. The metamorphic temperature was obviously high enough to force the homogenization of the inherited Ar component in these micas. This inherited Ar component is now detected as an excess component, but also the age is affected which is too high compared to the regional distribution of the cooling ages.

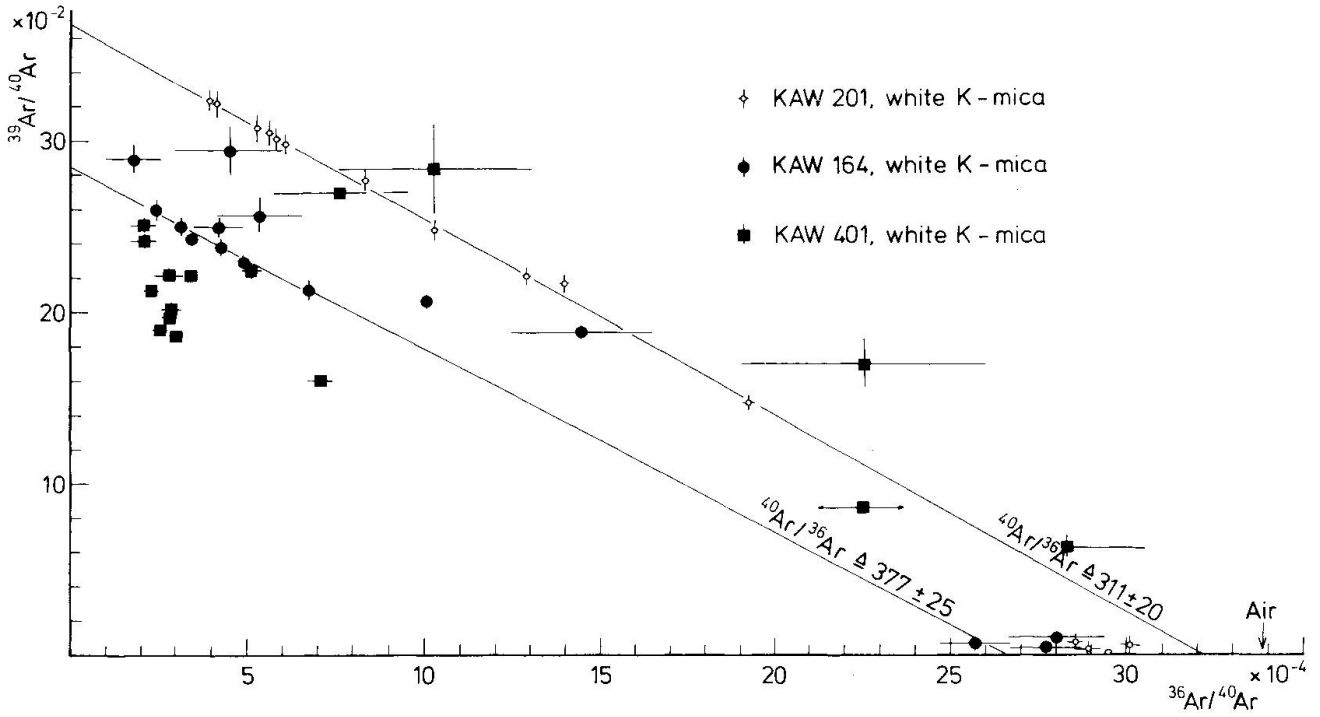

Fig. 8 Correlation diagram of $^{39}Ar/^{40}Ar$ vs $^{36}Ar/^{40}Ar$; the heating steps of KAW 164 between 995 and 1140 °C (Tab. 2) yield a straight line. The intercept on the x-axis points to an excess component. The data points of the well-defined plateau age (14.0 ± 0.3 Ma) of sample KAW 201 show a binary mixing line between an atmospheric component and the radiogenic ^{40}Ar and its parent isotope represented by the neutron induced ^{39}Ar. No correlation may be seen from the data of the hump-shaped spectrum of sample KAW 401.

In contrast, the heating steps of sample KAW 201 between 845 and 1200 °C give a regression line with a trapped component of which the $^{40}Ar/^{36}Ar$ ratio is equal to 311 ± 20. The corresponding age of 13.9 ± 0.3 Ma is comparable to the plateau age of 14.0 ± 0.3 Ma. Only this sample seems to be completely reset in respect to the meso-Alpine metamorphism, which led to temperature of 600 ± 20 °C. According to the criteria of LANPHERE and DALRYMPLE (1978) reviewed by DALRYMPLE et al. (1980), the plateau age of the white K-mica (KAW 201) seems to be meaningful.

WIJBRANS and MCDOUGALL (1986) have reported hump-shaped age spectra in a polymetamorphic terrain on the island Naxos (Greece). They concluded that the mechanical mixture of fine and coarse grained micas differing in age and in argon retentivities led to the hump-shaped age spectra. However, in our samples, the natural grain size found is quite uniform and matches the grain sizes of the analysed micas. Moreover, the phengite content in the white K-mica is randomly distributed in domains as shown by detailed microprobe analyses; therefore, we conclude that within individual minerals the chemical evolution from the eo-Alpine high pressure event to the meso-Alpine Barrow-type metamorphism is at least partly preserved.

In figure 9 the $^{37}Ar/^{39}Ar$ ratios of the samples KAW 401 and KAW 201 are plotted against the temperature of the particular heating step. The variation of this ratio is compared to the $^{40}Ar_{rad}/^{39}Ar$ ratio. The $^{37}Ar/^{39}Ar$ ratio should represent the K/Ca atomic ratio of the samples, according to the conversion of ^{39}K to ^{39}Ar by a (n,p)-reaction and of ^{40}Ca to ^{37}Ar by a (n,α)-reaction. For instance, HARRISON and FITZ GERALD (1986) found an antithetic variation between $^{40}Ar_{rad}/^{39}Ar$ and $^{37}Ar/^{39}Ar$ in hornblende. In contrast, results of single grain analysis of the K-feldspars (FOSTER et al., 1990) show only a weak correlation betwen age and $^{37}Ar/^{39}Ar$. In sample KAW 401 we also did not find a simple correlation between $^{40}Ar_{rad}/^{39}Ar$ and $^{37}Ar/^{39}Ar$, but it seems to be that the hump-shaped part of the age spectrum has higher $^{37}Ar/^{39}Ar$ ratios. This part of the spectrum is attributed to the phengite domains. These domains, however, have Ca contents below the detection limits of the microprobe and only domains with the same or larger diameter than the electron beam ($< 5 \cdot 10^{-3}$ mm) can be detected. The high $^{37}Ar/^{39}Ar$ ratios can be influenced by very small, but Ca-rich phengite domains. On the other hand, the chemical composition of the sample KAW 201 is very uniform and, surprisingly, the variation on the $^{37}Ar/^{39}Ar$ ratio does not correlate with the age. Therefore, the $^{39}Ar/^{37}Ar$ ratios ap-

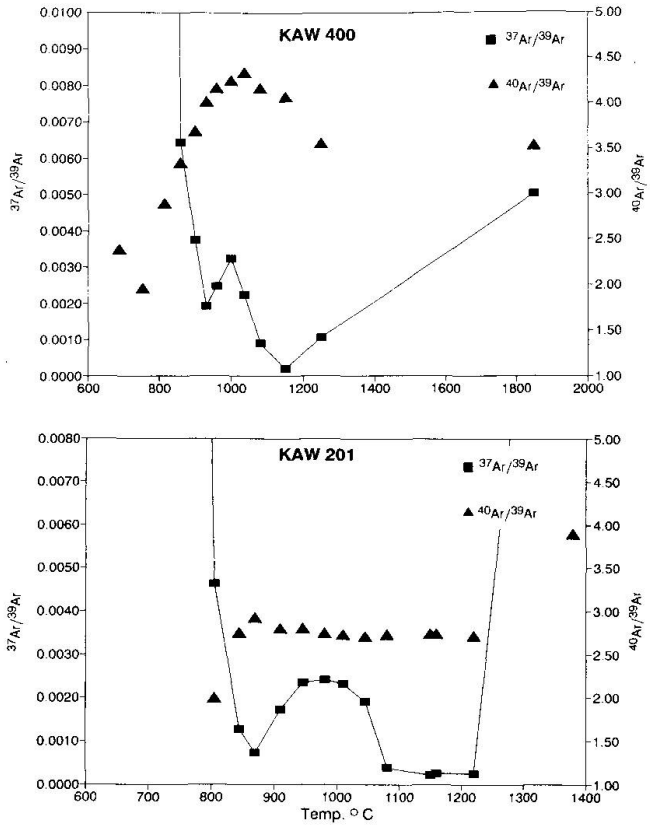

Fig. 9 The $^{37}Ar/^{39}Ar$ and the $^{40}Ar^{*}/^{39}Ar_K$ ratios are plotted against the temperature of the heating step. No correlation can be observed between the age reflecting ratio $^{40}Ar^{*}/^{39}Ar_K$ and the $^{37}Ar/^{39}Ar$ which refer to the Ca/K ratio either in the hump-shaped spectrum of sample KAW 401 or in the plateau age spectrum of sample KAW 201.

pears not to reflect the chemical composition of the white K-mica but the different diffusive behaviour of ^{39}Ar and ^{37}Ar during the extraction procedure. One reason for this might be the different locations of ^{39}Ar and ^{37}Ar in the crystal lattice.

CONCLUDING REMARKS

Along the cross section from Brig to Verampio p,T-conditions of meso-Alpine metamorphism are well defined deduced by petrological data of Mesozoic cover rocks (FRANK, 1983). They show a systematic increase in temperature and pressure from about 400 °C and 2 kbar to 600 °C and 6–8 kbar. Along the same profile, microprobe analyses on potassic white mica in granitic gneiss samples show that the phengite content of white K-mica in the assemblage Mu-Bi-Kfsp-Qz is clearly related to metamorphic grade. Using the geobarometer as calibrated by MASSONNE and SCHREYER (1987) the very high Si-content in sample KAW 401 (up to 7.2 Si per formula unit) indicates high formation pressures of about 13 kbar, reflecting conditions of eo-Alpine metamorphism. As a function of increasing metamorphic grade, a systematic evolution of potassic white mica composition from phengite to muscovite can be observed along the profile. In addition, a change in the structural polytypes from 3T to $2M_1$ is found. This result is in accordance with the study of FREY et al. (1983) who suggested an eo-Alpine origin for the 3T phengites as deduced from their regional distribution pattern in the Central Alps.

Strong and rather random variations of the Si-content in white K-mica samples KAW 401, 164, and 165 indicate local disequilibrium which is interpretated as "frozen-in" reaction textures. Complete equilibration was reached only in high grade samples in the Verampio area (muscovite of sample KAW 201) where meso-Alpine metamorphism exceeded temperatures of 580–620 °C.

The $^{40}Ar/^{39}Ar$ incremental degassing analyses reveal a systematic evolution of the age spectra, which again may be clearly related to metamorphic grade along the investigated profile:

– Potassic white mica samples from the northern part of the profile (KAW 401, 400, 164, 165), showing randomly distributed phengitic domains, gave typical hump-shaped age spectra (12–25 Ma) which decrease systematically with increasing metamorphic grade.

– At metamorphic temperatures above 580 °C (Verampio) the hump-shaped spectra disappear and muscovite sample KAW 210 gives a plateau age of 14.00 ± 0.30 Ma, which is interpreted as a cooling age.

The reason for the hump-shaped spectra is not simply caused by the mechanical mixture of two mica generation or the overgrowth of phengite by muscovite, as this would result in a staircase age pattern with increasing apparent ages at higher temperatures steps. Most probably, the reason is that relics of phengitic components are randomly distributed in the mica grains, as traced by our microprobe study, and survived the meso-Alpine event and thus were only partially degassed. Evidently, the meso-Alpine temperatures of 400–500 °C in the northern part of the cross-section were not high enough to reset the radiogenic system completely. To some extent the mineral reaction and reequilibration processes may be controlled to the migration behaviour of metamorphic fluids in these rocks as suggested by FRANK (1983). From evidence of different mica ages in different rock types within the same locality, we conclude that age resetting may be controlled to some extent by the grade of deformation and the type of the mineral reactions. Deformation induced recrystallization processes may have continued in the more

ductile Mesozoic cover rocks whereas they could have ceased much earlier in the granitic gneisses. The complete resetting of the K–Ar age in the Mesozoic rocks suggests open system behaviour in respect to Ar migration, whereas no complete Ar escape was possible in the closed system of the granitic gneisses.

Acknowledgements

We are indebted to Prof. Emilie Jäger for stimulating discussions at her laboratory. K.H. expresses gratitude to Professors P. Eberhardt and J. Geiss for use of the mass spectrometer equipment at the Physikalisches Institut, Bern. The work was supported financially by the Schweizerischer Nationalfonds zur Förderung der wissenschaftlichen Forschung and the Deutsche Forschungsgemeinschaft. The manuscript has benefited from detailed comments by Prof. H.J. Lippolt and useful suggestions by Prof. M. Frey.

References

BERGER, G.W. (1975): $^{40}Ar/^{39}Ar$ step heating of thermally overprinted biotite, hornblende and potassium feldspar from Eldora, Colorado. Earth Planet. Sci. Lett., 26, 387–408.

CHOPIN, CH. and MONIÉ, P. (1984): A unique magnesiochloritoid bearing, high-pressure assemblage from the Monte Rosa, Western Alps: petrologic and ^{39}Ar–^{40}Ar radiometric study. Contrib. Min. Petrol., 87, 388–398.

DALLMEYER, R.D. and GEE, D.G. (1986): $^{40}Ar/^{39}Ar$ mineral dates from retrogressed eclogites within the Baltoscandian miogeocline: Implication for a polyphase Caledonian orogenic evolution. Geol. Soc. Am. Bull., 97, 26–34.

DALRYMPLE, G.B., LANPHERE, M.A. and CLAGUE, D.A. (1980): Conventional and $^{40}Ar/^{39}Ar$ of volcanic rocks from Ojin (site 430), Nintoku (Site 432) and Suiko (Site 433) seamounts and the chronology of volcanic propagation along the Hawaiian Emperor chain. Init. Repts. Deep Sea Drill Proj., 55, 659–676.

DALRYMPLE, G.B., LANPHERE, M.A. and PRINGLE, M.S. (1988): Correlation diagrams in $^{40}Ar/^{39}Ar$ dating: is there a correct choice? Geophys. Res. Lett., 15, 6, 589–591.

FOLAND, K.A., LINDNER, J.S., LASKOWSKI, T.E. and GRANT, N.K. (1984): $^{40}Ar/^{39}Ar$ dating of glauconites: measured ^{39}Ar recoil loss from well-crystallized specimens. Isotope Geosci., 2, 241–264.

FLISCH, M. (1982): Potassium-argon analysis, in ODIN, G.S. (ed.): Numerical dating in stratigraphy, J. Wiley and Sons, 151–158.

FOSTER D.A., HARRISON, T.M., COPELAND, P. and HEIZLER, M.T. (1990): Effects of excess argon within large diffusion domains on K-feldspar age spectra. Geochimica et Cosmochimica Acta, 54, 1699–1708.

FRANK, E. (1979): Metamorphose mesozoischer Gesteine im Querprofil Brig–Verampio. Mineralogisch-petrographische und isotopengeologische Untersuchungen. Unpubl. Ph.D. Thesis, Universität Bern.

FRANK, E. and STETTLER, A. (1979): K–Ar and ^{39}Ar–^{40}Ar systematics of white K-mica from an Alpine metamorphic profile in the Swiss Alps. Schweiz. Mineral. Petrogr. Mitt., 59, 375–394.

FRANK, E. (1983): Alpine metamorphism of calcareous rocks along a cross-section in the Central Alps: occurrence and breakdown of muscovite, margarite and paragonite. Schweiz. Mineral. Petrogr. Mitt., 63, 37–93.

FREY, M., HUNZIKER, J.C., FRANK, W., BOQUET, J., DAL PIAZ, G., JÄGER, E. and NIGGLI, E. (1974): Alpine metamorphism of the Alps, a review. Schweiz. Mineral. Petrogr. Mitt., 54, 247–290.

FREY, M., HUNZIKER, J.C., JÄGER, E. and STERN, W.B. (1983): Regional distribution of white K-mica polymorphs and their phengite content in the Central Alps. Contrib. Mineral. Petrol., 83, 185–197.

FREY, M. and WIELAND, B. (1978): Chloritoid in autochthon-paraautochthonen Sedimenten des Aarmassivs. Schweiz. Mineral. Petrogr. Mitt., 55, 407–418.

GILLESPIE, A.R., HUNEKE, J.C., and WASSERBURG, G.J. (1983): Eruption age of a Pleistocene basalt from ^{40}Ar–^{39}Ar analysis of partially degassed xenoliths. Jour. Geophys. Res., 88, 4997–5008.

GILLESPIE, A.R., HUNEKE, J.C. and WASSERBURG, G.J. (1984): Eruption age of a ≈ 100.000-year-old basalt from ^{40}Ar–^{39}Ar analysis of partially degassed xenoliths. Jour. Geophys. Res., 89, 1033–1048.

GUIDOTTI, C.V. and SASSI, F.P. (1976): Muscovite as a petrogenetic indicator mineral in Pelitic schists. N. Jb. Min. Abh., 127, 97–142.

HALL, W.D.M. (1972): The structural and metamorphic history of the lower pennine nappes, Val di Bosco, Ticino, Switzerland. Ph.D. Theses, London.

HAMMERSCHMIDT, K. (1982): K/Ar and $^{40}Ar/^{39}Ar$ age resolution from illites of the Trias of Mauls; Mesozoic cover of the Austroalpine basement, Eastern Alps (South Tyrol), Schweiz. Mineral. Petrogr. Mitt., 62, 113–133.

HANSON, S.N., SIMMONS, K.R. and BENCE, A.E. (1975): ^{40}Ar–^{39}Ar spectrum age for biotite, hornblende and muscovite in a contact metamorphic zone. Geochim. Cosmochim. Acta, 39, 1269–1277.

HARRISON, T.M. and MCDOUGALL, I. (1980): Investigations of an intrusive contact, northwest Nelson, New Zealand – I. Thermal, chronological and isotopic constraints. Geochim. Cosmochim. Acta, 44, 1985–2003.

HARRISON, T.M. and FITZ GERALD, J.D. (1986): Exsolution in hornblende and its consequences for $^{40}Ar/^{39}Ar$ age spectra and closure temperature. Geochim. Cosmochim. Acta, 50, 247–253.

HESS, J.C. and LIPPOLT, H.J. (1986) : Kinetics of Ar isotopes during neutron irradiation: ^{39}Ar loss from minerals as a source of error in $^{40}Ar/^{39}Ar$ dating. Isotope Geosci., 59, 223–236.

HURFORD, A.J. and HAMMERSCHMIDT, K. (1985): $^{40}Ar/^{39}Ar$ and K/Ar dating of the Bishop and Fish Canyon Tuffs: Calibration ages for fission-track dating standard. Chem. Geol., 58, 23–32.

HUNEKE, J.C. and SMITH, S.P. (1976): The realities of recoil: ^{39}Ar recoil out of small grains and anomalous age patterns in ^{39}Ar–^{40}Ar dating. Proc. Seventh Lunar Sci. Conf. Geochim. Cosmochim. Acta Suppl., 1987–2008.

HUNZIKER J.C. and BEARTH P. (1969): Rb-Sr-Altersbestimmungen aus den Walliser Alpen. Biotitalterswerte und ihre Bedeutung für die Abkühlgeschichte der alpinen Metamorphose. Eclogae geol. Helv., 62, 205–222.

JÄGER, E., NIGGLI, E. and WENK, E. (1967): Rb-Sr-Al-

tersbestimmungen an Glimmern der Zentralalpen. Beitr. Geol. Karte der Schweiz, NF Liefg. 134, Kümmerly + Frey, Bern.

JESSBERGER, E.K. (1982): Die $^{40}Ar/^{39}Ar$-Altersbestimmungstechnik: Prinzipien, Entwicklungen und Anwendungen in der Kosmochronologie. Chem. Erde, 41, 40–94.

KÖPPEL, V. and GRÜNENFELDER, M. (1978): The significance of monazite U–Pb ages: Examples from the Lepontine area of the Swiss Alps. In "Fourth International Conference of Geochronology, Cosmochronology and Isotope Geology", Abstracts, Denver, 226–227.

LANPHERE, M.A. and DALRYMPLE, G.B. (1976): Identification of excess ^{40}Ar by the $^{40}Ar/^{39}Ar$ age spectrum technique. Earth Planet. Sci. Lett., 32, 141–148.

LOVERA, O.M., RICHTER, F.M. and HARRISON, T.M. (1989): The $^{40}Ar/^{39}Ar$ thermochronometry for slowly cooled samples having a distribution of diffussion domain sizes. Jour. Geophys. Res., 94, B12, 17919–17935.

MASSONNE, H.-J. and SCHREYER, W. (1987): Geobarometry based on the limiting assemblage with K-feldspar, phlogopite, and quartz. Contrib. Mineral. Petrol., 96, 212–224.

MAURER, P. (1973): $^{40}Ar/^{39}Ar$-Kristallisationsalter und $^{37}Ar/^{38}Ar$-Strahlungsalter von Apollo 11-, 12- und 17-Steinen und dem Apollo 17-"orange soil". Thesis, University of Berne.

MILNES, A.G. (1974): Post-nappe folding in the Western Lepontine Alps. Eclogae geol. Helv., 67, 333–348.

MILNES, A.G., GRELLER, M. and MÜLLER, R. (1981): Sequence and style of major post-nappe structures, Simplon-Pennine Alps. Jour. Struct. Geol., 3, 411–420.

NIGGLI, E. and NIGGLI, C.R. (1965): Karten der Verbreitung einiger Mineralien der alpidischen Metamorphose in den Schweizer Alpen. Eclogae geol. Helv., 58, 355–368.

ONSTOTT, T.C. and PEACOCK, M.W. (1987): Argon retentivity of hornblendes: a field experiment in a slowly cooled metamorphic terrane. Geochim. Cosmochim. Acta, 51, 2891–2903.

PURDY, J. and JÄGER, E. (1976): K–Ar ages on rock-forming minerals from the Central Alps. 1st Geol. Min. Univ. Padova., 30, 1–31.

RADICATI DI BROZOLO, F., HUNEKE, J.C., PAPANASTASSION, D.A. and WASSERBURG, G.J. (1981): ^{40}Ar–^{39}Ar and Rb–Sr age determinations on Quaternary volcanic rocks. Earth Planet. Sci. Lett., 53, 445–456.

RODDICK, J.C., CLIFF, R.A. and REX, D.C. (1980): The evolution of excess argon in alpine biotites – A ^{40}Ar–^{39}Ar analysis. Earth Planet. Sci. Lett., 48, 185–208.

ROSS, J.A. and SHARP, W.D. (1988): The effect of subblocking temperature metamorphism on the K/Ar systematics of hornblendes: $^{40}Ar/^{39}Ar$ dating polymetamorphic garnet amphibolites from the Franciscan Complex, California. Contrib. Mineral. Petrol., 100, 213–221.

STECK (1987): Le massif du Simplon – Réflexions sur la cinématique des nappes de gneiss. Schweiz. Mineral. Petrogr. Mitt., 67, 27–45.

STEIGER, R.H. and JÄGER, E. (1977): Subcommission on geochronology: Convention on the use of decay constants in geo- and cosmochronology. Earth Planet. Sci. Lett., 36, 359–362.

STETTLER, A., EBERHARD, P., GEISS, J., GRÖGLER, N. and MAURER, P. (1973): $^{39}Ar/^{40}Ar$ ages and $^{37}Ar/^{38}Ar$ exposure ages of lunar rocks. Proc. IV. Lun. Sci. Conf. (Suppl. IV, Geochim. Cosmochim. Acta), 2, 1865–1888.

TROMMSDORFF, V. (1966): Progressive Metamorphose kieseliger Karbonatgesteine in den Zentralalpen zwischen Bernina und Simplon. Schweiz. Mineral. Petrogr. Mitt., 46, 431–460.

TRÜMPY, R. (1980): Geology of Switzerland. A guide book Part A: An outline of the Geology of Switzerland. 104 S., Wepf & Co Publishers Basel, New York.

TURNER, G., CADOGAN, P.H. and YONGE, C.J. (1973): Argon selenochronology. Proc. IV. Lun. Sci. Conf. (Suppl. IV, Geochim. Cosmochim. Acta), 2, 1889–1914.

VANCE, D.C. and O'NIONS, K.R. (1991): Constraints on prograde and retrograde alpine thermal histories from precise garnet chronometry. Terra abstacts, 3, 436.

WIJBRANS, R.R. and MCDOUGALL, I. (1986): $^{40}Ar/^{39}Ar$ dating of white micas from an Alpine high-pressure metamorphic belt on Naxos (Greece): the resetting of the argon isotopic system. Contrib. Mineral. Petrol., 93, 187–194.

Manuscript received September 9, 1990; revised manuscript accepted June 12, 1991.